UNIVERSITY OF CALIFORNIA

Radiation Laboratory

BERKELEY, CALIFORNIA

DISCLAIMER

UCRL-2756 Rev.

UNIVERSITY OF CALIFORNIA
Radiation Laboratory
Berkeley, California

Contract No. W-7405-eng-48

$C^{12}(x, xn)C^{11}$ AND $Al^{27}(x, x2pn)Na^{24}$ CROSS SECTIONS AT HIGH ENERGIES

Walter E. Crandall, George P. Millburn, Robert V. Pyle
and Wallace Birnbaum

July, 1955

Printed for the U. S. Atomic Energy Commission

$C^{12}(x, xn)C^{11}$ AND $Al^{27}(x, x2pn)Na^{24}$ CROSS SECTIONS AT HIGH ENERGIES

Walter E. Crandall,* George P. Millburn, Robert V. Pyle, and Wallace Birnbaum*

Radiation Laboratory,
University of California,
Berkeley, California

July, 1955

ABSTRACT

The $C^{12}(x, xn)C^{11}$ and $Al^{27}(x, x2pn)Na^{24}$ cross sections were measured for protons (105 to 350 Mev), deuterons (85 to 190 Mev), and alpha particles (380 Mev) by using a 4π β counter to determine the absolute disintegration rate and measuring the incident flux with a Faraday cup. The absolute value of the $C^{12}(p, pn)C^{11}$ excitation function was found to be 13 percent lower than the value previously published for these energies, and was found to be constant between 200 and 350 Mev. The new value of this reaction cross section removes some of the discrepancies between p-p scattering cross sections measured elsewhere and those measured at Berkeley, and affects other experiments that use the reaction as a proton flux monitor. The other cross sections are in reasonable agreement with values determined by comparable methods.

The relative excitation functions for $C^{12}(d, dn)C^{11}$ and $C^{12}(He^3, He^3n)C^{11}$ reactions were also measured by a stacked-foil technique using end-window counters. These were normalized to absolute values from the 4π counter data for detuerons.

---

* Now at the University of California Radiation Laboratory, Livermore, California.

$C^{12}(x, xn)C^{11}$ AND $Al^{27}(x, x2pn)Na^{24}$ CROSS SECTIONS AT HIGH ENERGIES

Walter E. Crandall*, George P. Millburn, Robert V. Pyle, and Wallace Birnbaum

Radiation Laboratory,
University of California,
Berkeley, California

July, 1955

I. INTRODUCTION

Absolute cross sections for reactions producing C^{11} and Na^{24} from bombardment of C^{12} and Al^{27} with high-energy particles have been determined for protons of 105 to 350 Mev, deuterons of 85 to 190 Mev, and alpha particles of 380 Mev, by use of the external beams of the 184-inch cyclotron. Many of the excitation functions have been determined previously, some by essentially the same technique used in this experiment,[1,2,3,4,5] but because of the importance of these reaction cross sections for beam monitoring[6,7,8] it was decided to redetermine the absolute values separately. An important feature of the experiment was the nearly concurrent measurement of all the cross sections, which should help insure high accuracy of the ratios.

The method involved absolute determination of the number of particles impinging on the targets by use of a Faraday cup, and absolute determination of the disintegration rate by use of a 4π, constant-flow, methane proportional counter calibrated against a similar instrument of the National Bureau of Standards,** and against β-γ coincidence counting. Corrections for self-absorption in the foils were empirically determined.

---

* Now at the University of California Radiation Laboratory, Livermore, California.

** We are indebted to Dr. H. H. Seliger of the Radioactivity Section of the National Bureau of Standards for his assistance in providing us with sources previously calibrated in their 4π β counter.

Besides a desire to redetermine the absolute cross sections in view of recent advances in absolute β counting, an incentive for the experiment was the discrepancy in the shape of the $C^{12}(p, pn)C^{11}$ excitation function near 350 Mev as reported by two different groups.[1,2] Two methods of degrading the proton energy were used to explore the reasons for the discrepancy. The same technique was applied to the $C^{12}(d, dn)C^{11}$ excitation function near the maximum available energy (190 Mev). The $C^{12}(\alpha, \alpha n)C^{11}$ and $Al^{27}(x, x2pn)Na^{24}$ reaction cross sections were measured only for the maximum particle energies.

In an experiment which preceded the bulk of the work being reported, the relative excitation functions for the $C^{12}(d, dn)C^{11}$ and $C^{12}(He^3, He^3n)C^{11}$ reactions were measured by a stacked-foil technique. An end-window counter was used in these experiments and the results were normalized from the 4π counter data for deuterons. Although the precision of these measurements was low compared with the other cross sections, the values were included for completeness.

The following discussions relate only to the techniques and procedures used in the 4π counter experiments; discussion of the end-window counter data is reserved for the end of the paper.

II. EXPERIMENTAL PROCEDURE

A. Beam Characteristics and Monitoring

A plan view of the cyclotron is shown in Fig. 1. Most of the measurements were made with the scattered external beam which emerged from the magnetic deflectors, passed over the proton probe cart, through the premagnet collimator, through the steering magnet, and then through the 48-inch collimator and into the experimental area (cave). All the beams used were monoergic to within one percent.

The beam was monitored by a Faraday cup.[1] The signal from the cup was led to one of several low-leakage Fast condensers which had been calibrated against a similar condenser measured by the National Bureau of Standards to within 0.1 percent.* Measurements made with different condensers showed

---

* We are indebted to A. H. Scott and C. Peterson of the Electricity Division of the National Bureau of Standards for assistance in obtaining the calibration.

excellent agreement. The voltage on the condenser was measured by a 100 percent inverse-feedback integrating electrometer and a Speedomax recorder, which were calibrated against a Rubicon potentiometer to within 0.1 percent.

The charge collected by the Faraday cup must be related to the number of particles that passed through the target foils. Factors that must be considered in the measurement of the beam include secondary emission (electrons or heavy charged particles) from the face of the cup, high-energy secondary particles emitted forward from the thin foil (0.005 in. Be-Cu) in the face of the vacuum housing, loss of charge by conduction through the cup supports and residual gas in the cup housing, and the relative area of the foils and the cup compared to the spatial distribution of the beam.

Previous experience with the Faraday cup used in this experiment showed that a thin foil biased to ± 300 volts had a negligible effect on the collection characteristics of the cup when it was used in the experimental area shown in Fig. 1. Presumably the stray magnetic field (~25 gauss) in this area was more effective than a biasing voltage applied to the foil. An additional magnetic field (~100 gauss) produced no observable change in the collection efficiency of the cup. Thus secondary emission from the face of the cup was not an important source of error.

Teflon insulators were used throughout the collection system with a resulting time constant for the entire system of many days. The gas pressure in the cup chamber had to be increased to more than 100 microns before ionization of the gas by the beam was observable. Conduction losses were minimized by maintaining the cup close to ground potential through the action of the feedback amplifier.

The spatial distribution of the beam was investigated by exposing an array of plastic scintillators (CH) diametrically across the beam. The C^{11} activity was essentially constant near the center and then dropped rapidly to less than 10^{-4} of the activity of the central region. If the activity in the region beyond the rapid fall-off is attributed to a neutron flux, then the correction (1.25 percent) for the portion of the charged particle beam collected by the cup that did not pass through the target foils was almost precisely cancelled by the correction for the neutron flux.

The largest correction to the Faraday cup readings resulted from the high-energy electrons emitted from the vacuum-housing foil.*

The number of electron collisions in a copper foil of thickness t mg/cm^2 is determined by the Rutherford scattering cross section,

$$N_e = \int_{x_1}^{t} dx \int_{0}^{\theta_{max}} 1.37 \times 10^{-4} \frac{z^2 t}{\beta^4} \frac{d \cos \theta}{\cos^3 \theta}$$

per incident particle of charge z with velocity βc. The maximum energy of the electrons is (4m/M)E for an incident particle of mass M and energy E (non-relativistically). Not all the electrons escape from the foil because of their finite range and multiple scattering. By neglecting the latter effect and assuming the electron range to be well defined (i.e., a sharp drop to zero intensity at a unique thickness), one may calculate a maximum correction. In Table I the results of such calculations are tabulated assuming the electron ranges to be

Table I

Calculated number of high-energy electrons in the forward direction from 0.005-in. copper foil

Particle	Effective Electron Range in Units of Extrapolated Ranges		
	1.0 $R_{ext.}$	0.7 $R_{ext.}$	0.5 $R_{ext.}$
350-Mev proton	0.020	0.019	0.016
205 " "	0.030	0.023	0.016
170 " "	0.033	0.023	0.016
190-Mev deuteron	0.039	0.028	0.020
105 " "	0.040	0.029	0.020
85 " "	0.041	0.030	0.020
380-Mev alpha	0.13	0.092	0.067

* The magnitude of this effect was called to our attention by the article on p-p scattering at 460 Mev, by Meshcheryakov, Bogachev, Neganov, and Piskarev, Ac. Sci. Doklady, U.S.S.R. 99, 995 (1954) (Reference 9).

1.0, 0.7, and 0.5 of the extrapolated ranges.[10] The curves for number vs. absorber thickness may be approximated by straight lines, so the mean range is half the extrapolated range. Therefore we have chosen to use the calculations for half the extrapolated range, and, in order to take into account the multiple scattering, we have arbitrarily applied only one-half the calculated correction. We assign an uncertainty in the beam monitoring equal to the applied correction.

B. Degradation of Particle Energy

Carbon absorbers placed in front of the target foils in the path of the beam were used to degrade the incident energy. The particle current that emerged from the absorbers was contaminated with relatively low-energy particles, which were thought to be the cause of the discrepancies mentioned above in the shape of the $C^{12}(p, pn)C^{11}$ excitation function near 350 Mev.[2] Absorbers were placed in two positions in an attempt to measure the effect of the secondary particles. Position A was directly before the Faraday cup, so that the particles emerged from the absorber and passed through the target foils into the Faraday cup. This was essentially the technique used by Aamodt et al.[1] to degrade the proton energy. Because the $C^{12}(x, xn)C^{11}$ cross section increases for energies lower than those used in this experiment, the effect of low-energy secondary particles on the excitation function is magnified in relation to their number. Absorbers were also placed in position B, which was on the proton probe cart (Fig. 1) in the path of the scattered beam. The collimators and steering magnet then provided a good energy selector, and low-energy charged particles were no longer present in the beam entering the cave. Absorbers were also placed at position A in these experiments to obtain further energy degradation and to study the effect of the secondary particles as a function of the incident-particle energy.

Actually, several absorbers were used at position A and target foils were placed at various depths. The Faraday cup then measured the current through the last foil. To determine the current (primary plus charged secondary particles) that passed through the other foils in the absorber, separate measurements were made with an ionization chamber in front of the absorber. The same absorbers used above were then in turn inserted between the chamber and the Faraday cup to measure the fraction I/I_o of the beam that passed through foils placed at the various depths in the absorber. This technique gave the total particle

current at each foil position to an accuracy comparable with the direct measurement of the incident current, since measurements at 350 Mev with and without absorber in the beam path gave the same value for the cross section.

In analogy to the geometries defined in scattering experiments, measurements made with the absorbers at position A are referred to as "poor geometry" measurements, while those at position B are referred to as "good geometry" measurements.

C. Foils

The carbon foils were made of polystyrene, $(CH)_n$ and were 1 or 1.25 in. in diameter. The thicknesses varied from 1 to 15 mils. Some of the foils were coated with very thin layers (of the order of 100 angstroms) of silver to test the effect of nonconducting samples on the efficiency of the 4π proportional counter as described below. The aluminum foils were of the same diameters and 5 and 10 mils thick.

Each of the target foils represented a slice of a "thick" slab of the foil material. "Guard" foils of 5 mils thickness were placed between foils of different elements and between foils and absorbers to protect against recoil loss and capture.[11,12] In addition, several foils were usually stacked at each absorber depth, and no variation in apparent cross section was observed in these foils.

The beam diameter was 0.5 in. when the 1-inch-diameter foils were used, and 0.75 in. when the 1.25-inch-diameter foils were used. The foils were large enough to intercept essentially all the beam, including the multiply scattered portion. This was shown by inserting photographic film at each absorber depth; the blackening was always confined to an area less than that of the foils. The small fraction of the beam that may have missed the foils was compensated by the effects of the neutron contamination as shown by a beam distribution survey described in Section IIA.

The foils were weighed and measured to an accuracy of about 0.1 percent. The foils were counted for 3 or more half lives; the C^{11} activity fitted best a 20.4-min. half life, and the Na^{24} a 15.1-hr. half life.

D. 4π Proportional Counter

The target foils were counted in a 4π constant-flow methane proportional counter.[13] A typical voltage plateau is shown in Fig. 2. No discriminator plateaus were taken because the discriminator was fixed internally at a point above the noise level. The operation of such a counter has been described by Seliger and Cavallo.[13]

Since the field is low at the sample position when nonconducting foils are counted,[13] several polystyrene foils were coated with silver to a thickness of approximately 100 angstroms (measured by the comparative light transmission of coated and uncoated foils). There was never any significant difference between the determinations of the cross section with an uncoated foil and those with a coated foil, which indicates that essentially all the β particles were energetic enough to escape the low-field region. This problem did not enter when aluminum foils were used.

The efficiency of the counter as a function of foil diameter and foil position was also investigated. Aluminum foils varying from 0.25 to 1.5 in. in diameter were activated in a uniform neutron flux and the relative counting rate per unit weight showed no variation as a function of foil diameter within the statistical uncertainty (~1 percent). Also a small test foil was counted at various distances from the foil holder and no dependence on position existed in the region occupied by the foils (Fig. 3).

Long-lived, β-active isotopes mounted on thin foils were used to check the performance of the counter during the period of the experiments.

To check the efficiency of the 4π counter against a suitable standard, three sources calibrated by the National Bureau of Standards were obtained.* Two were Tl^{204} sources and one was a Sr^{90}-Y^{90} source. The sources were sandwiched between 0.2 mg/cm^2 of aluminum leaf to prevent source losses, and the NBS calibration was made after sandwiching. The ratios of the counting rates in our counter compared with those in the NBS counter were 0.99, 1.00, and 1.01; we therefore believe the counter to be 100 ± 1 percent as efficient as the NBS counter, which is at least 99 percent efficient.[13]

E. Self-Absorption

In view of the preceding discussion, the major uncertainty in the absolute beta counting was the self-absorption in the activated foils. To determine a useful self-absorption curve required measurement of high precision, which in turn required a minimum number of measured parameters. The following factors entered into these measurements:

(1) Time between measurements should be as short as possible to minimize decay corrections.

---

* Courtesy of Dr. H. H. Seliger, NBS.

(2) The counting rate should be as high as possible to eliminate background uncertainties.

(3) Better than 1 percent statistics required.

(4) Counting rate should remain almost constant to maintain dead-time correction nearly constant.

(5) The weight of the foil should not enter critically in the measurement.

(6) The uniformity of the foil activation should not enter critically into the measurement.

(7) The foil geometry should not be important.

To minimize the uncertainty from the first three factors a high counting rate was required, which aggravated the correction due to dead time. For comparing thin foils, uncertainties from factors (5) and (6) became appreciable. Two techniques were used to minimize these effects. A technique which removed most uncertainties, except factor (7), was to use a single thin foil which was counted and then folded and recounted in exactly the same counting arrangement. In this case there was a slight reduction in counting rate due to the increased thickness of the doubled foil, since the other factors remained unchanged. This procedure was repeated for increased thickness with increased uncertainties due to edge effects. To eliminate the edge effects, but with uncertainties in the dead-time corrections, uniformly activated foils were counted singly and then combined so that weighing and activation uncertainties were small.

To further reduce the uncertainties in the 4π counter measurements, the absolute disintegration of several activated foils was measured by the beta-gamma coincidence technique. In this case the activated foils were sandwiched between plastic scintillators placed on the end of a photomultiplier for the beta counting, and the gamma counting was done with a NaI scintillator. The beta efficiency was approximately 90 per cent and the gamma efficiency roughly 3 percent. Slight corrections for γ-γ coincidences (0.5 percent) and dead-time (1 percent) were applied. The agreement between 4π counting and the β-γ counting was good, but in the case of the polystyrene foils the β-γ point appeared to be slightly higher than the extrapolation of the 4π counting data to zero thickness. Since both measurements have systematic uncertainties of the order of this difference, the self-absorption curves were normalized to a point midway between the two zero-point determinations.

The self-absorption curve for uniformly activated polystyrene is shown in Fig. 4. The curve should apply to any measurement of the C^{11} activity in foils where the activated area is more than a range of the beta particles from the foil edge. In high-energy bombardment, the production of Be^{7} in the foil requires that the foils be counted less than 2.5 hours after bombardment for the contaminating activity from Be^{7} to be less than 1 percent. The similar curve for Na^{24} activity in aluminum is shown in Fig. 5. In this case contamination by F^{18} and Na^{22} require that the measurements be made more than 18 hours but less than 3.5 days after bombardment to be free from contaminating activity. In particular, the Na^{22} activity, with its low-energy betas, has a much steeper self-absorption curve and can produce large uncertainties in the measurements.

III. RESULTS

A. Energy Dependence of Cross Sections

The measurements of the $C^{12}(x, xn)C^{11}$ cross sections as a function of energy showed a significant dependence on the position of the absorber in relation to the target foil. Measurements made in "poor geometry" (position A) consistently gave apparent cross sections about 7 percent higher than those measured in "good geometry" (position B). This dependence was ascribed to the charged and uncharged secondary particles that leave the absorber. (A crude calculation of the effects agreed very well with the empirical corrections.)

Figure 6 shows the apparent variation of the $C^{12}(p, pn)C^{11}$ cross section as a function of the proton energy. Measurements for three different incident beam energies are shown (the incident energy was varied by placing absorbers in position B, and the variation of the cross section with energy was determined by placing absorbers in position A). In each case the cross sections are normalized to the value at the incident beam energy. All the curves show the rise found in earlier experiments,[1] and it would appear that the increase is a consequence of the method of beam degradation rather than a true nuclear effect, for the cross section for the "good geometry" measurements is essentially constant.

The ratio of the apparent cross section as a function of absorber thickness is shown in Fig. 7. The points are an average of the data shown in Fig. 6, with the lowest-energy point (170 Mev) omitted (since at this energy the cross section appears to show a significant increase). The conclusion drawn from Fig. 7 is

that the secondary particles increase the observed cross section in a constant ratio for absorbers greater than a given thickness. The effect of the secondaries does not continue to increase as the absorber thickness increases because

(1) the low-energy secondary particles are scattered, and a fraction, which increases with absorber thickness, misses the foil;

(2) the relatively low-energy charged secondary particles are removed by ionization loss within a short distance from their creation; and

(3) the secondary particles are emitted with an angular distribution so that a large fraction of those formed in the front of the absorber miss the foil.

The results of these measurements would seem to remove the discrepancy mentioned in the introduction in the shape of the excitation function, and would require that the excitation function reported in Reference 1 be corrected for energies below the maximum beam energy.

Similar behavior is exhibited by the $C^{12}(d, dn)C^{11}$ excitation function, although the details are different because deuteron and proton interactions give different energy and angular distributions for the secondary particles.

The excitation function for $C^{12}(a, an)C^{11}$ was not measured, but somewhat similar behavior probably should be expected.

B. Absolute Values of the Cross Sections

The absolute values of the cross sections were calculated from the formula

$$\sigma = \frac{A_{oo}}{\lambda} \frac{1}{N} \frac{A}{A_o t},$$

where A_{oo}/λ is the number of reactions produced by N particles in a foil with $A_o t/A$ nuclei per unit area. The last quantity was calculated from the measured weights and diameters of the foils; the first, from the decay constant λ and the measured counting rates corrected for decay and self-absorption; the second, from the charge collected by the Faraday cup corrected for high-energy electrons. No correction was applied for neutron-induced events and the fraction of the beam collected by the Faraday cup that missed the foils, because these two effects cancelled each other. The cross sections measured in "poor geometry" were corrected by the empirically determined factors for the effects of secondary particles; for protons the correction was a uniform reduction of 1/1.07; for deuterons, a reduction of 1/1.04 for 0.5-in. carbon absorbers and 1/1.08 for greater thicknesses. The correction may be significantly in error for the lower deuteron energies because the absorbers were relatively thick

compared with the ranges. All energy measurements were based on the Aron et al.[14] range curves. None of the cross sections was corrected for the isotopic abundance.

As an additional check on the beam-monitoring technique, the $C^{12}(p, pn)C^{11}$ cross section was measured for 340-Mev protons by bombarding 1 x 1 x 0.75-in. plastic scintillator (effectively polystyrene) in a uniform proton flux. Ilford G.5 emulsions were placed on each side of the scintillator and proton tracks were counted to determine the particle flux. The C^{11} activity was counted by placing the scintillator in optical contact with a photomultiplier tube and the counting efficiency was determined by the β-γ coincidence technique. This measurement gave a cross section of 36 ± 3 mb.

The ratio of the $C^{12}(p, pn)C^{11}$ and $Al^{27}(p, 3pn)Na^{24}$ cross sections was measured by the simultaneous bombardment of a sandwich of aluminum and polystyrene foils at 340 Mev and was found to be 3.21, in agreement with the ratio of the absolute cross sections determined independently.

C. Errors

The absolute cross sections are listed in Table II with their associated relative standard errors. The values quoted are subject to various systematic errors, some of which have been discussed above. They include

(1) self-absorption		± 3 percent
(2) condenser and electrometer calibration	<	± 1 percent
(3) counter efficiency		+ 1 percent
(4) secondary particle effect		± 2 percent
(5) knock-on electrons		± 1 to ± 4 percent (Table I)
(6) beam spatial distribution		+ 1.25 percent
(7) neutron contamination		- 1.25 percent
(8) half-life uncertainty	<	± 1 percent

An estimate of the accuracy of our measurements is + 5 and - 4 percent for 350-Mev protons and 190-Mev deuterons.

D. Comparison with Other Measurements

Also listed in Table II are results of previously published values of the absolute cross sections. With the exception of the $C^{12}(p, pn)C^{11}$ cross section, all our values are as much as 20 percent larger than those previously reported. Full discussions of the techniques and corrections applied to these measurements were not given, so it is difficult to assess the severity of the discrepancies. It should be noted that essentially the same beam-monitoring techniques were

Table II

Absolute reaction cross sections
(4π counter data only)

	Particle Energy (Mev)	Geometry	Cross Section* (mb)
A. $C^{12}(p, pn)C^{11}$	350	good	36.0 ± 0.7
	320	good	35.5 ± 0.7
	325	poor	35.9 ± 0.8
	295	good	37.9 ± 0.4
	295	poor	35.5 ± 1.0
	270	poor	35.9 ± 1.0
	240	poor	37.2 ± 1.8
	204	poor	37.0 ± 2.0
	170	poor	39.7 ± 0.9
B. $C^{12}(d, dn)C^{11}$	190	good	61.1 ± 0.6
	180	good	60.8 ± 0.6
	180	poor	60.6 ± 1.3
	160	good	60.6 ± 0.9
	160	poor	61.3 ± 1.3
	145	poor	60.6 ± 1.8
	130	poor	61.6 ± 1.8
	105	poor	60.7 ± 1.0
	85	poor	56.9 ± 1.8
C. $C^{12}(\alpha, \alpha n)C^{11}$	380	good	57.0 ± 0.6
	380	good	48 ± 3 [a]
D. $Al^{27}(p, 3pn)\ Na^{24}$	350	good	11.1 ± 0.2
	420	....	10.8 ± 0.5 [b]
E. $Al^{27}(d, 3p2n)Na^{24}$	190	good	28.8 ± 0.3
	190	good	22 ± 2 [c]
F. $Al^{27}(\alpha, 4p3n)Na^{24}$	380	good	24.2 ± 0.3
	380	good	23.4 [a]

[a] See Ref. 3

[b] See Ref. 6

[c] See Ref. 5

* Note: All errors are standard errors of a single measurement and do not include estimated uncertainties due to possible systematic effects. Corrections for self-absorption, geometry, and knock-on electrons have been made. See text.

used in all the experiments, and that corrections for the knock-on electrons from the Faraday cup housing foil were not applied to the previous measurements.

Recently Rosenfeld et al[15] have redetermined the $C^{12}(p, pn)C^{11}$ cross section at 460 Mev and quote 33 mb as a preliminary value, in reasonable agreement with our results. Also recent measurements up to 2.9 Bev[16] of the ratio of the $C^{12}(p, pn)C^{11}$ and $Al^{27}(p, 3pn)Na^{24}$ cross sections are in reasonable agreement with our results.

The most significant difference from earlier experiments is the shape of the $C^{12}(p, pn)C^{11}$ excitation curve in the neighborhood of 350 Mev (Fig. 8). Readjusting the excitation function both in shape and absolute value will have important effects on seemingly unrelated experiments because of the widespread use of the reaction as a beam monitor. For example, the p-p scattering cross sections measured at 240 Mev by Oxley et al[8] should certainly be modified. Even though they intercalibrated their counter with a beta standard used by Aamodt et al., the revised shape of the excitation function requires a 41/49 reduction in their values (to 4.05 ± 0.32 mb/ster.). If a cross section of 36.0 mb for the $C^{12}(p, pn)C^{11}$ reaction is used, their values are further reduced (to 3.56 ± 0.28 mb/ster.) and are in excellent agreement with the results of Chamberlain et al.[17] (3.6 ± 0.2 mb/ster.).

The p-p scattering cross sections measured by Birge et al[8] at 105 and 75 Mev may be reduced directly by the ratio 36/41 (to 4.6 ± 0.9 and 5.8 ± 1.2 mb/ster, respectively). The revised values are in agreement with the Berkeley measurements.[17]

Cassels et al[8] measured the p-p scattering cross sections at 146 Mev by using two methods to calibrate their beam monitor. One of the methods involved the use of the $C^{12}(p, pn)C^{11}$ cross section and gave a p-p scattering cross section of 4.61 ± 0.55 mb/ster. This result should be reduced in the ratio 43/57 to 3.56 ± 0.42 mb/ster. Their value based on a photographic emulsion calibration remains high compared with other measurements.

E. End-Window Counter Measurements

The stacked-foil technique was used to measure the relative excitation functions of deuterons and He^3 particles for the $C^{12}(x, xn)C^{11}$ reaction. Graphite foils 1-11/16 in. in diameter and 1/8 and 1/16 in. thick were placed between guard foils and inserted at various depths in uranium absorbers.

Near the end of the range, the carbon foils were inserted consecutively. The incident-particle current was measured by an ionization chamber and the current through each foil was determined from charge-attenuation curves measured with a Faraday cup.[18]

The foils were counted in an end-window β counter with a 3.5-mg/cm^2 window. The counter and its use in connection with these experiments are described more fully in a paper by Schecter et al.[19] No activity other than the 20.4-minute C^{11} was observed; the foils were counted for several half lives. Corrections were applied for counter dead time, C^{11} decay, and geometry differences (found empirically).

The excitation curve for deuterons was normalized to the high-energy point from 4π counter data, and the low-energy cross sections were corrected for secondary particles as in Section IIB. The range of the deuterons was determined for a similar stack and the energies were computed from the tables of Aron et al.[14] Uncertainties in the range point cause the large energy uncertainties for low energies; the horizontal lines in Fig. 9 represent an estimate of the uncertainty in placement of the midpoint, and do not represent merely the spread (due to range straggling) of energies that pass through the foil.

The excitation function for He^3 particles shown in Fig. 10 was normalized on the basis of the deuteron data, because both curves were measured under the same experimental conditions. The techniques and corrections were the same for both cases; for the cross sections shown in Fig. 10, a constant correction of 1/1.08 was applied to the data for energies lower than the maximum. The errors on the points are unsymmetrical because it was felt that such a correction for secondary-particle effects was very likely incorrect for incident He^3 particles. The inelastic and stripping cross sections for He^3 are approximately equal to those for deuterons,[18] but the stripped secondaries have ranges greater than the residual range of the He^3 particle.[18] Thus the effects of the secondary particles may not level off to a constant value as quickly as they do for protons and deuterons whose secondaries have ranges shorter than the residual range of the primary particle. Caution should be exercised in use of the data of Fig. 10, for the measured shape of the excitation function may be incorrect. The cross section within experimental error for energies greater than 80 Mev.

IV. SUMMARY AND CONCLUSIONS

In addition to obtaining absolute values of the cross sections, we have measured the ratios of the various reaction cross sections with a good degree of accuracy, certainly to less than 5 percent. In addition we have shown that the $C^{12}(x, xn)C^{11}$ excitation functions are nearly constant at and near the maximum energies of the charged-particles beams available at Berkeley; earlier measurements that indicated a sharp dip near the maximum energy underestimated the effect of secondary particles produced in the attenuators.

The absolute value of the $C^{12}(p, pn)C^{11}$ cross section at 350 Mev is significantly lower than that reported earlier,[1] and the difference is believed to be due to the increased accuracy of absolute β-counting that has been achieved in the last few years. Readjustment of the excitation function on the basis of our results leads to improved agreement between the p-p scattering cross sections measured at Berkeley and those measured elsewhere[8] using the $C^{12}(p, pn)C^{11}$ reaction to monitor the proton beam. The reported results of other experiments will be affected by the readjustment of the excitation function; a partial list of such experiments is given in References 6 to 8.

ACKNOWLEDGMENTS

The authors are happy to acknowledge the support and assistance of Dr. C. M. VanAtta. We also wish to thank Frank L. Adelman, John Ise, Jr., Larry Schecter, Marian N. Whitehead, Donald A. Hicks, and Robert M. Main for assistance in collecting data, and the cyclotron crew under the direction of James Vale for helpful cooperation. Joe Murray and Nahmin Horwitz assisted in the β-γ coincidence measurements.

This work was done under the auspices of the U. S. Atomic Energy Commission.

1. R. Aamodt, V. Peterson and R. Phillips, Phys. Rev. 88, 739 (1952); W. W. Chupp and E. M. McMillan, Phys. Rev. 72, 873 (1947).
2. S. D. Warshaw, R. A. Swanson, and A. H. Rosenfeld, Phys. Rev. 95, 649(A) (1954).
3. M. Lindner and R. N. Osborne, Phys. Rev. 91, 1501 and 342 (1953).
4. P. C. Stevenson, H. G. Hicks, and R. L. Folger, to be published in the Physical Review.
5. R. E. Batzel, W. W. T. Crane, and G. D. O'Kelley, Phys. Rev. 91, 939 (1953).
6. L. Marquez, Phys. Rev. 88, 225 (1952); Phys. Rev. 86, 405 (1952).
7. E. Belmont and J. M. Miller, Phys. Rev. 95, 1554 (1954).
8. p-p and p-d scattering cross sections affected by the change in the $C^{12}(p, pn)C^{11}$ excitation curve are: R. W. Birge, V. E. Kruse, and N. F. Ramsey, Phys. Rev. 91, 885 (1953); C. L. Oxley, R. D. Shamberger, and O. A. Towler, Phys. Rev. 78, 326 (1950); 84, 1262 (1951); 85, 416 (1952); 85, 1024 (1952); J. B. Cassels, T. G. Pickavance, and G. H. Stafford, Proc. Roy. Soc. (London) 214, 262 (1952). Other experiments affected include: J. W. Meadows, Phys. Rev. 91, 885 (1953); K. Strauch and J. A. Hoffman, Phys. Rev. 86, 563 (1952); 90, 449 (1953); L. Marquez and I. Perlman, Phys. Rev. 81, 953 (1951).
9. Mescheryakov, Bogachev, Neganov, and Piskarev, Doklady Akad. Nauk, S. S. S. R. 99, 995 (1954).
10. H. A. Bethe and J. Askin, "Experimental Nuclear Physics," Vol. I, E. Segre, Ed., Wiley and Sons, 1953.
11. R. E. Batzel and G. T. Seaborg, Phys. Rev. 82, 607 (1951).
12. S. Fung and I. Perlman, Phys. Rev. 87, 623 (1952).
13. H. H. Seliger and L. Cavallo, NBS J. Research 47, 41 (1951); also H. H. Seliger and A. Schwebel, Nucleonics 12, 54 (July, 1954).
14. W. A. Aron, B. G. Hoffman, and F. C. Williams, AECU-663.
15. A. H. Rosenfeld, private communication.
16. R. F. Wolfgang and G. Friedlander, Phys. Rev. 96, 190 (1954); and erratum to be published.
17. O. Chamberlain, E. Segre, and C. Wiegand, Phys. Rev. 83, 932 (1951).

18. G. P. Millburn, W. Birnbaum, W. E. Crandall, and L. Schecter, Phys. Rev. 95, 1268 (1954), and unpublished data.

19. L. Schecter, W. E. Crandall, G. P. Millburn, and J. Ise, Jr., Phys. Rev. 97, 184 (1955).

CAPTIONS

Fig. 1 Plan view of the cyclotron showing the path of the scattered beam. Absorbers for the "good geometry" experiments were placed on the proton probe cart and interposed in the scattered beam at position B; the steering-magnet current was then adjusted so that only particles of the proper energy entered the cave.

Fig. 2 Typical high-voltage plateau for the 4π proportional counter.

Fig. 3 The active foils were inserted into the 4π counter on a probe as shown in the figure. The geometrical sensitivity of the counter was tested with a small test foil and the relative sensitivity is shown in the lower half of the figure. The active foil was always confined to the region of uniform sensitivity.

Fig. 4 The fraction of the C^{11} decay positrons escaping from a uniformly activated polystyrene foil is plotted against the foil thickness. The curve is arbitrarily normalized to the mean value of the β-γ coincidence measurement and the extrapolation of the 4π measurements to zero thickness.

Fig. 5 The fraction of the Na^{24} decay betas escaping from a uniformly activated aluminum foil is plotted against the foil thickness. The curve is arbitrarily normalized to the mean value of the β-γ coincidence measurement and the extrapolation of the 4π measurements to zero thickness.

Fig. 6 The apparent $C^{12}(p, pn)C^{11}$ cross section from "poor geometry" measurements is plotted against proton energy for three different incident proton energies. The apparent rise at lower energies is due to secondary interactions in the attenuator (see text).

Fig. 7 The apparent increase in the $C^{12}(p, pn)C^{11}$ cross section due to secondary interactions is plotted versus absorber thickness in the "poor geometry" measurements.

Fig. 8 The excitation function for the $C^{12}(p, pn)C^{11}$ reaction is plotted as a function of proton energy. The dots are "good geometry" measurements, and the triangles are "poor geometry" measurements, corrected as described in the text. The squares are from the data of Reference 1 normalized to 36.0 mb at 350 Mev.

Fig. 9 The excitation function for the $C^{12}(d, dn)C^{11}$ reaction is plotted as a function of the deuteron energy. The dots are "good geometry" measurements, and the triangles are "poor geometry" measurements, corrected as described in the text. The squares are the end-window counter data normalized at 190 Mev to the 4π counter data.

Fig. 10 The excitation function of the $C^{12}(He^3, He^3n)C^{11}$ reaction is plotted as a function of the He^3 energy. The measurements were made with an end-window counter whose efficiency was determined relative to the 4π counter through the normalization of the 190-Mev deuteron data. The correction for secondary interactions at less than the maximum energy is very uncertain and is reflected in the unsymmetrical errors.

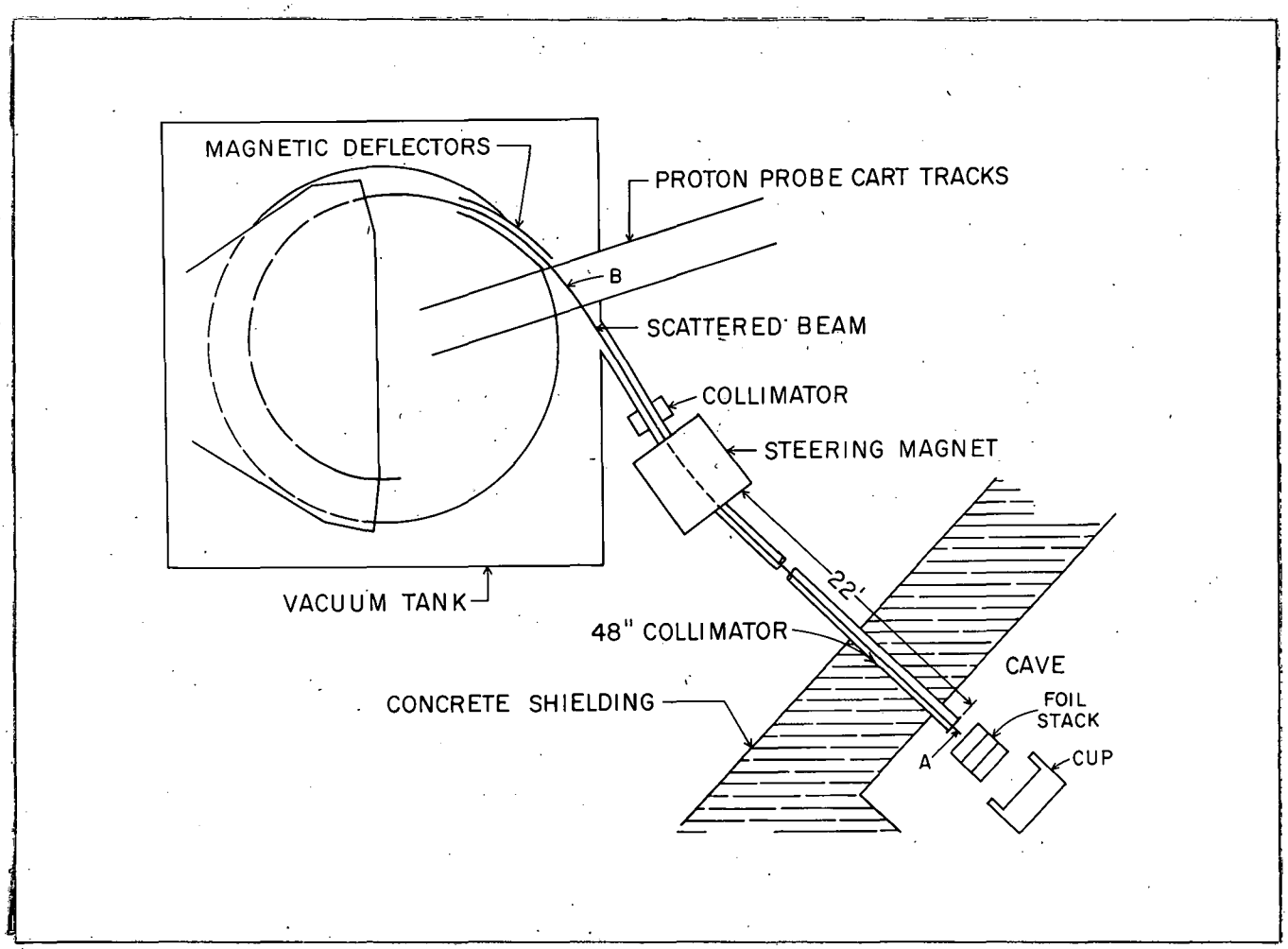
MAGNETIC DEFLECTORS
PROTON PROBE CART TRACKS
B
SCATTERED BEAM
COLLIMATOR
STEERING MAGNET
22'
VACUUM TANK
48" COLLIMATOR
CAVE
CONCRETE SHIELDING
FOIL STACK
A
CUP

Fig. 1

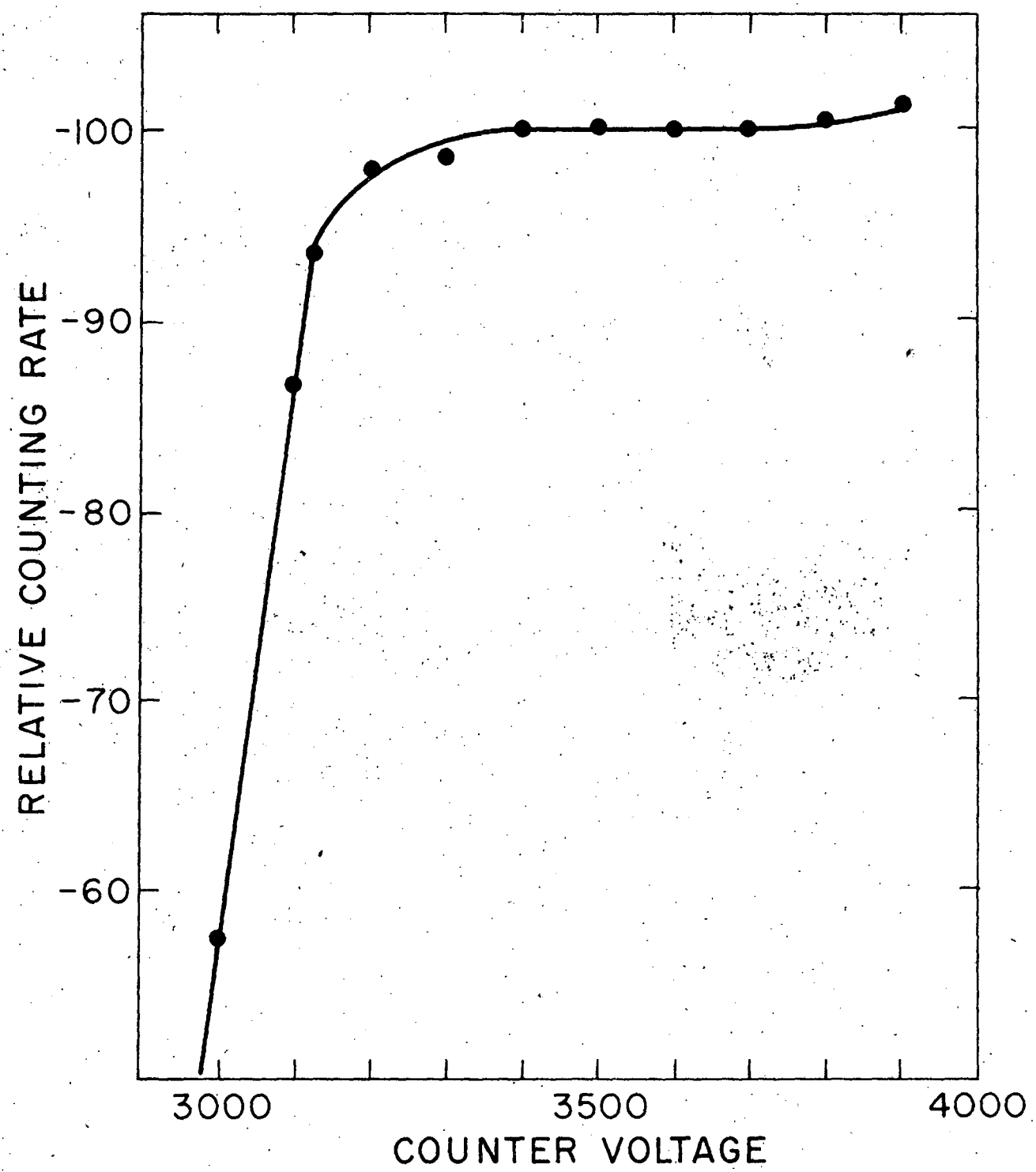
-100
-90
-80
-70
-60
RELATIVE COUNTING RATE
3000
3500
4000
COUNTER VOLTAGE

Fig. 2

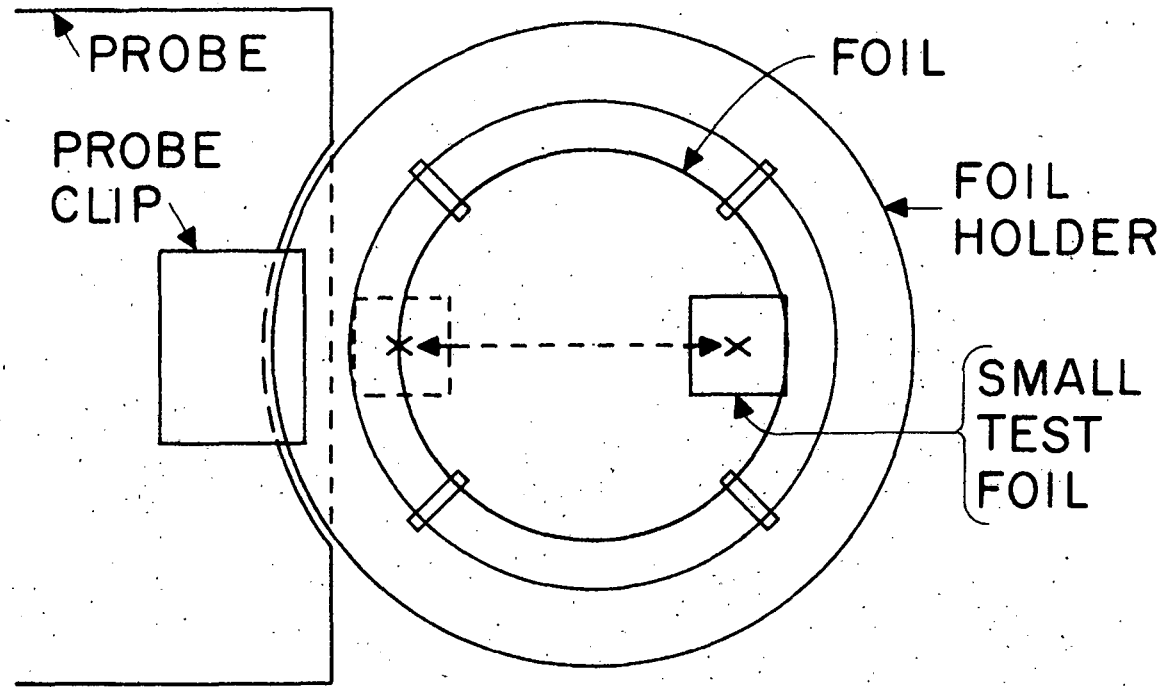

TYPICAL LOCATION OF FOIL AND FOIL HOLDER IN CLIP ON PROBE

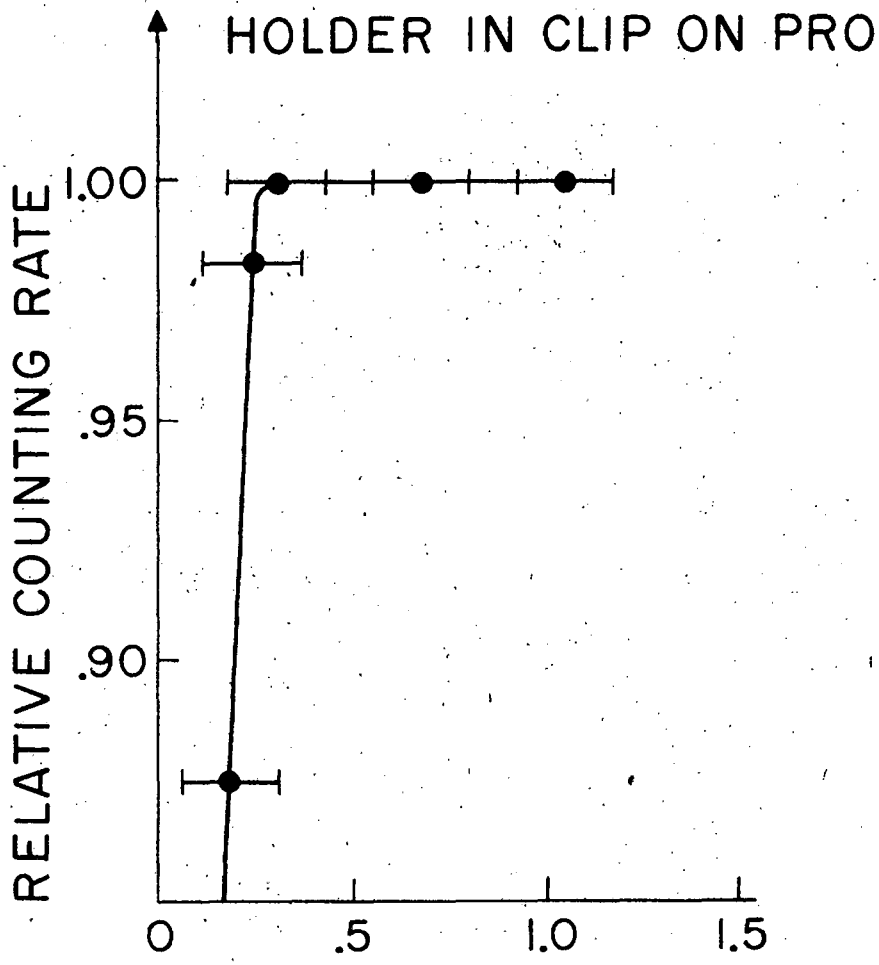

Fig. 3
23260-1

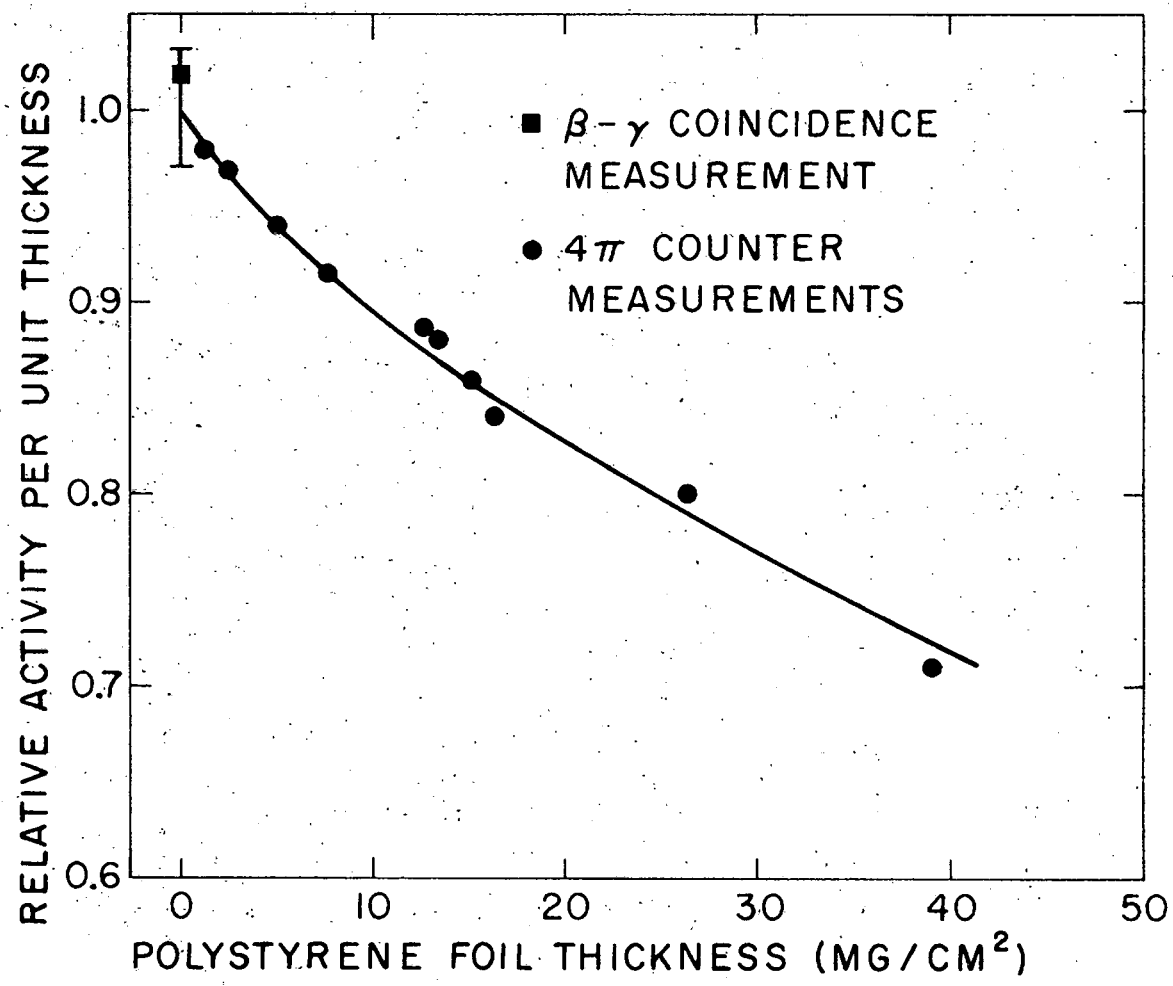
RELATIVE ACTIVITY PER UNIT THICKNESS
1.0
0.9
0.8
0.7
0.6
0
10
20
30
40
50
POLYSTYRENE FOIL THICKNESS (MG/CM²)
β-γ COINCIDENCE MEASUREMENT
4π COUNTER MEASUREMENTS

Fig 4

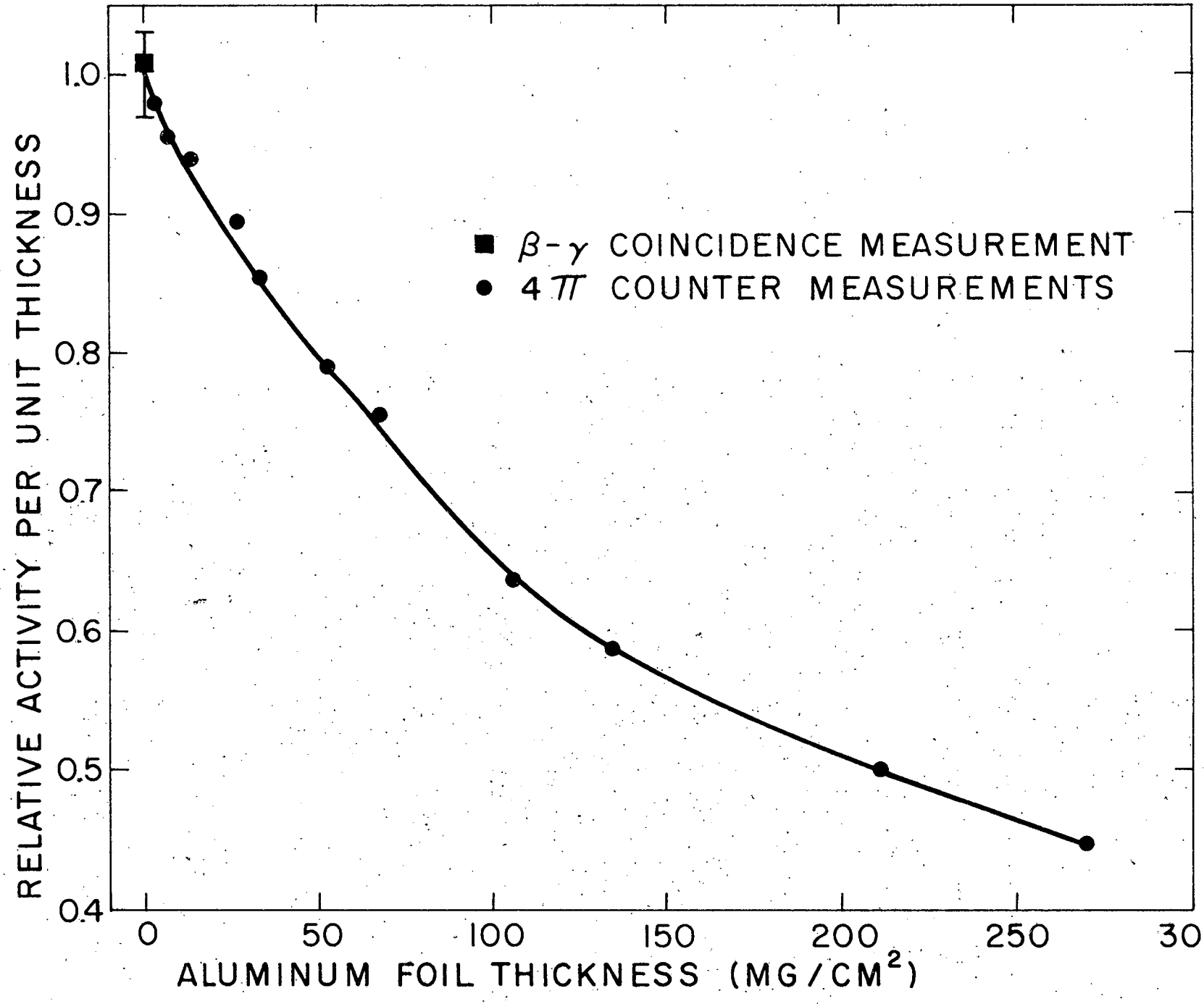
RELATIVE ACTIVITY PER UNIT THICKNESS
1.0
0.9
0.8
0.7
0.6
0.5
0.4
0
50
100
150
200
250
300
ALUMINUM FOIL THICKNESS (MG/CM²)
β-γ COINCIDENCE MEASUREMENT
4π COUNTER MEASUREMENTS

Fig. 5

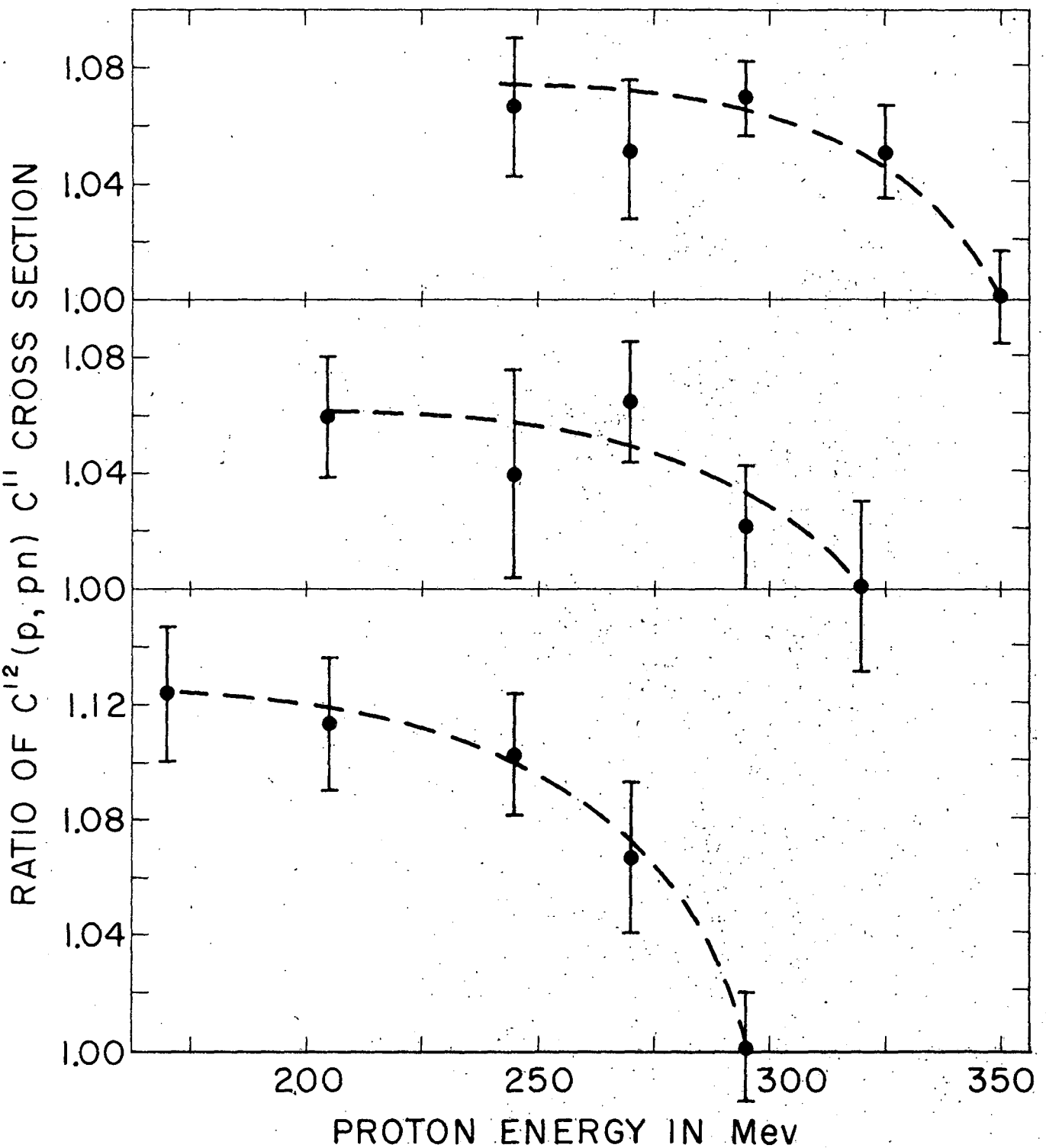
RATIO OF $C^{12}(p, pn)\, C^{11}$ CROSS SECTION
1.08
1.04
1.00
1.08
1.04
1.00
1.12
1.08
1.04
1.00
200
250
300
350
PROTON ENERGY IN Mev

Fig. 6

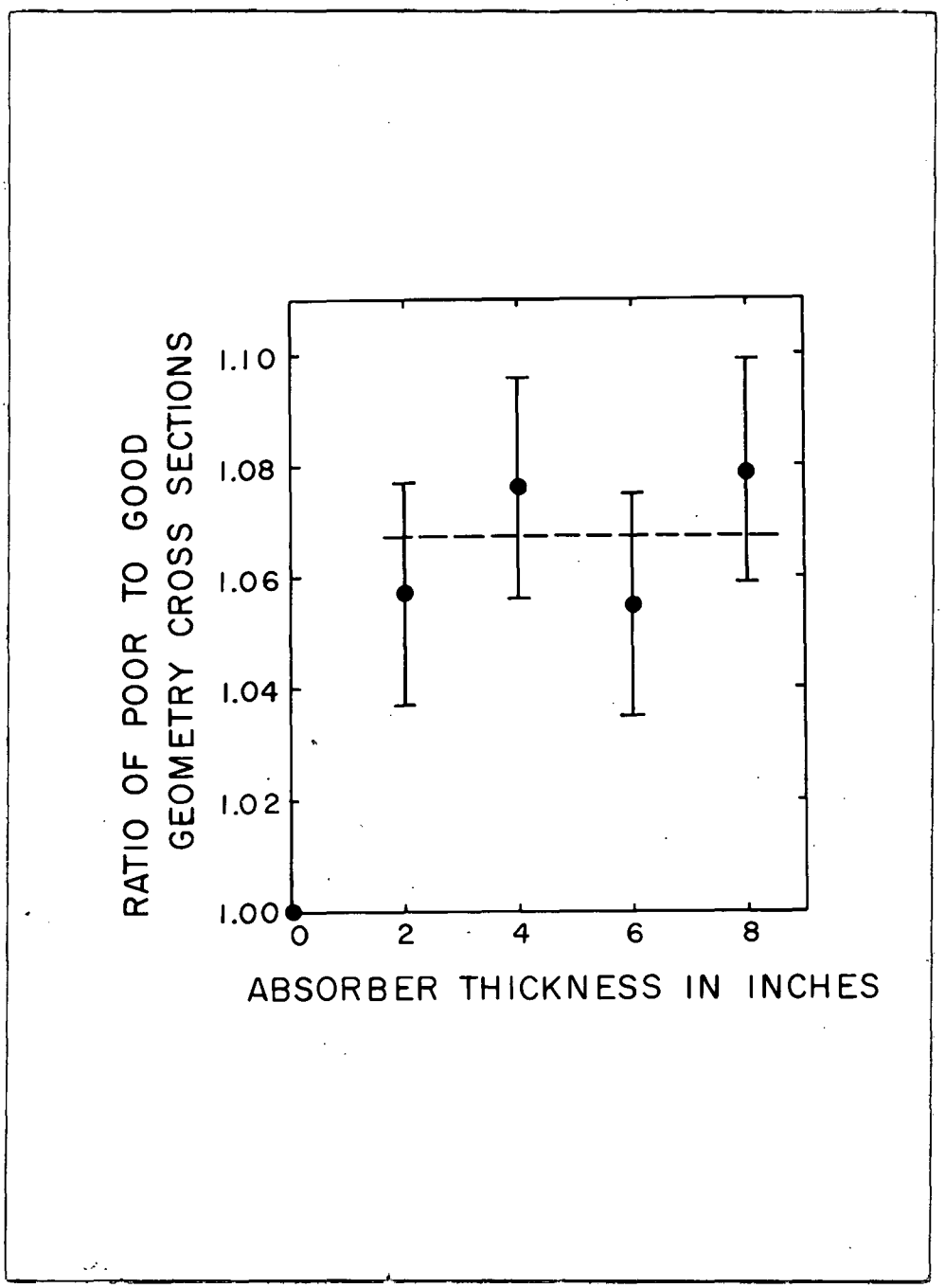
RATIO OF POOR TO GOOD
GEOMETRY CROSS SECTIONS
1.10
1.08
1.06
1.04
1.02
1.00
0
2
4
6
8
ABSORBER THICKNESS IN INCHES

Fig. 7

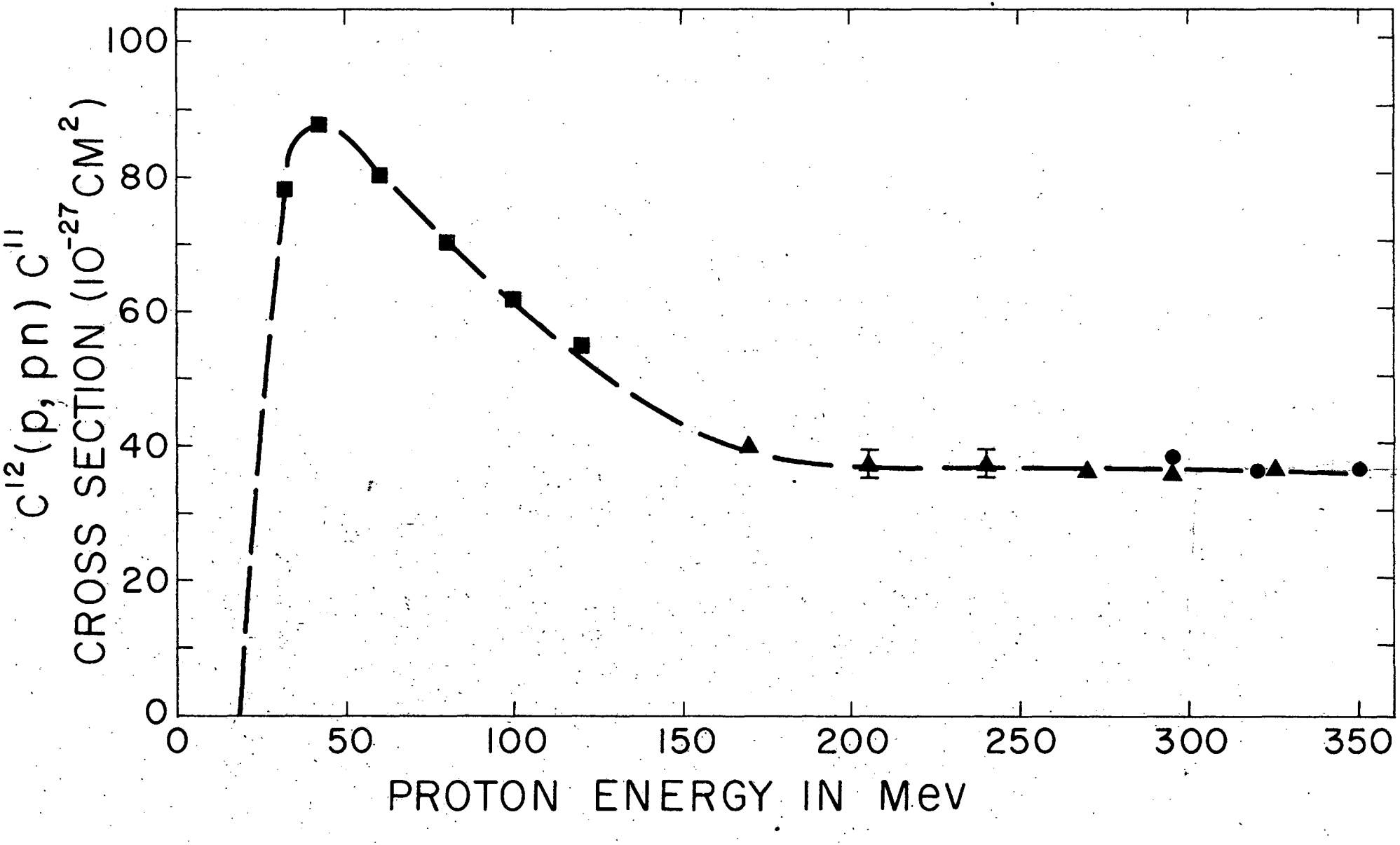
$C^{12}(p, pn)\, C^{11}$
CROSS SECTION (10^{-27} CM^2)
100
80
60
40
20
0
0
50
100
150
200
250
300
350
PROTON ENERGY IN Mev

Fig. 8

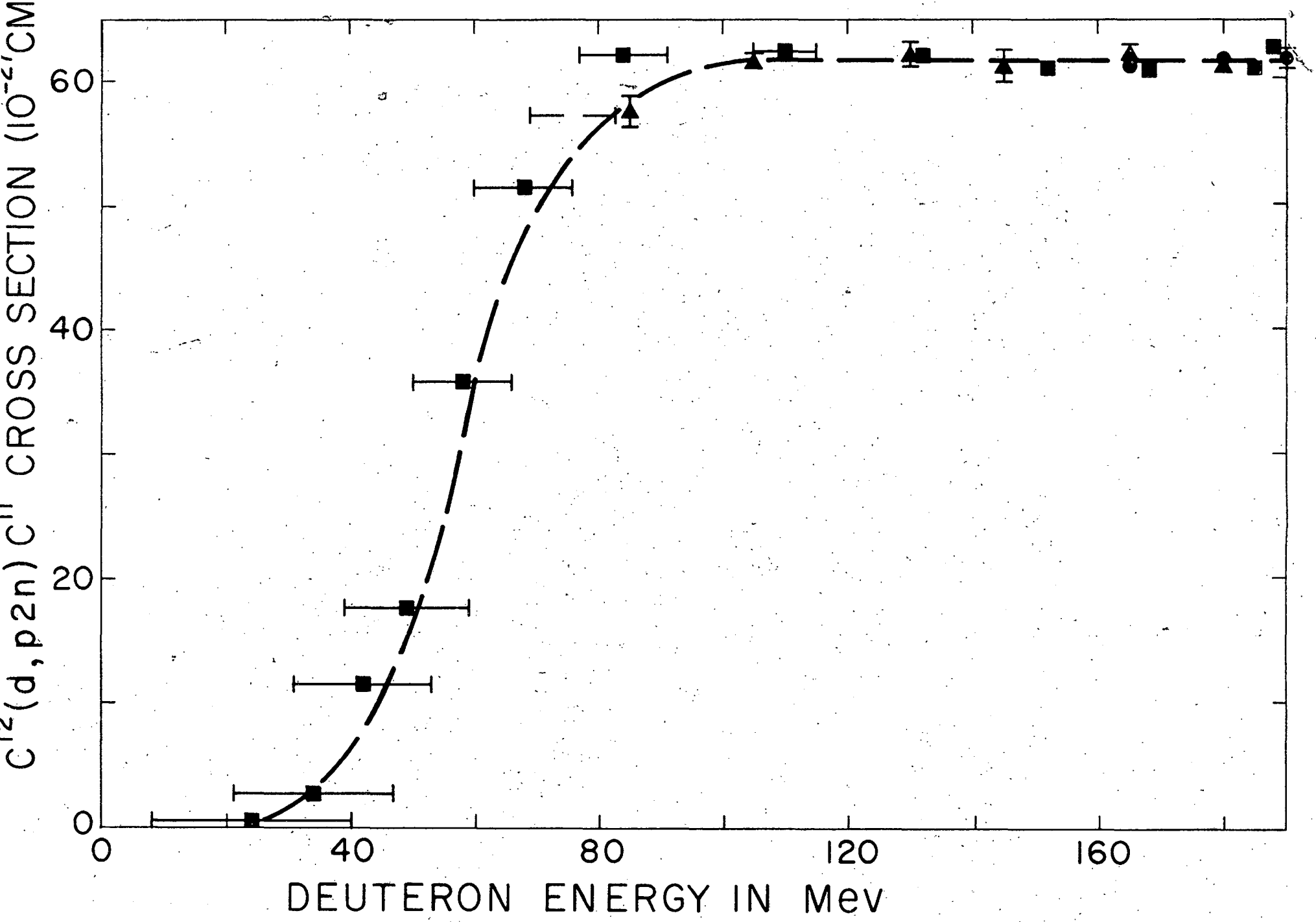
$C^{12}(d,p2n)C^{11}$ CROSS SECTION (10^{-27}CM
0
20
40
60
0
40
80
120
160
DEUTERON ENERGY IN Mev

Fig. 9
23264-1

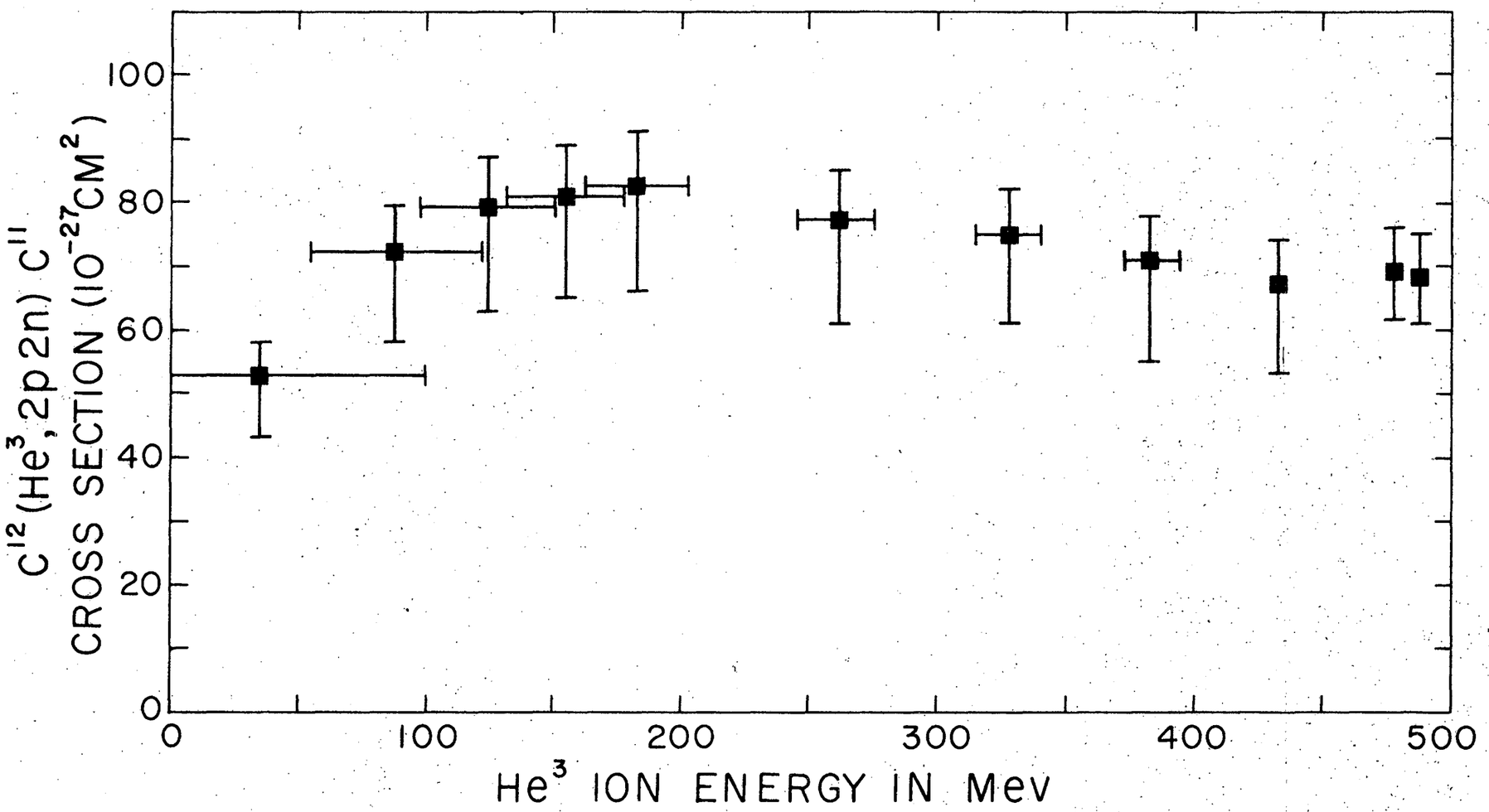
$C^{12}(He^3,2p2n)\,C^{11}$
CROSS SECTION ($10^{-27}CM^2$)
100
80
60
40
20
0
0
100
200
300
400
500
He^3 ION ENERGY IN Mev

Fig. 10